# Ultra-Wideband Phase Shifters

Amin M. Abbosh

***Abstract*—A method with clear guidelines is presented to design compact planar phase shifters with ultra-wideband (UWB) characteristics. The proposed method exploits broadside coupling between top and bottom elliptical microstrip patches via an elliptical slot located in the mid layer, which forms the ground plane. A theoretical model is used to analyze performance of the proposed devices. The model shows that it is possible to design high-performance UWB phase shifters for the 25°–48° range using the proposed structure. The method is used to design 30° and 45° phase shifters that have compact size, i.e., 2.5 cm × 2 cm. The simulated and measured results show that the designed phase shifters achieve better than ±3° differential phase stability, less than 1-dB insertion loss, and better than 10-dB return loss across the UWB, i.e., 3.1–10.6 GHz.**

***Index Terms*—Aperture coupling, phase shifter, ultra-wideband (UWB).**

## I. Introduction

PHASE shifters are common microwave devices, which are widely used in electronic beam-scanning phased arrays, microwave instrumentation and measurement systems, modulators, and many other industrial applications. In these and many other applications, and in order to get wideband performance, phase shifters are usually realized in planar (stripline or microstrip) technology due to its nondispersive and broadband propagation properties.

In order to achieve the broadband operation of the phase shifters, the approach of coupled transmission lines is usually employed. One of the earliest designs that used the coupled lines method to construct broadband phase shifters is the Schiffman differential phase shifter [1]. It consists of two transmission lines: the reference transmission line and the folded edge-coupled section. By the proper selection of the length of these lines and the degree of coupling, the phase difference between them can be made constant at 90° over a broadband. However, Schiffman's original study was based on stripline transmission structures, where the odd and even modes propagating along the coupled lines have equal phase velocities. When this type of circuit is designed in a microstrip form, the unequal odd- and even-mode velocities results in poor performance [2]. Moreover, the measured results of Schiffman's phase shifter indicate a high phase ripple $(\pm 10^{\circ})$ [1].

In order to obtain a broader bandwidth with an acceptable phase ripple using the edge-coupled method, some authors proposed the use of cascaded multiple coupled sections [3]–[7]. Shelton and Mosko [4] described an approximate synthesis technique for fixed phase shifters consisting of multiple parallel-coupled quarter-wave sections. The main drawback of this procedure, which is general to edge-coupled shifters, is that in order to achieve a broadband, an extremely tight coupling is required, which may not be realizable in a given practical configuration. Shelton and Mosko [4] proposed the use of tandem coupling to minimize the effect of this problem. However, tandem configuration requires wire crossovers, which is inconvenient from the manufacturing point of view. The designed configuration in [4] suffers from another serious problem, which is the large size required for the multiple coupled sections.

In order to decrease the size of the multisection coupling structure required in the design presented in [4], an optimization technique was used to calculate parameters of the edge-coupled broadband phase shifter [5]. The structure considered in [5] consists of a cascade of coupled line pairs of varying length and coupling coefficients and each connected together at one end. The main drawback of the adopted technique is that it still requires a large number of coupled line pairs to achieve the required phase performance.

Some other modifications were proposed to improve performance of the edge-coupled structures using new forms of multisection coupling lines [6] and a double or parallel Schiffman phase shifter [7]. However, the design presented in [6] requires a very narrow slot (tens of micrometers), which makes the fabrication process very difficult. Moreover, the measured phase performance presented in [6] shows a phase shifter that covers only the $C$-band (4–8 GHz) with a phase error of $\pm 6.5^{\circ}$. The circuit presented in [7] (referred to as a double parallel Schiffman) consists of two parallel-connected coupled sections designed to yield a 90° phase difference. The lengths and coupling values are adjusted to obtain a desired phase ripple. The measured results of the design in [7] indicate a narrowband performance with high phase instability at the lower and higher ends of the frequency band.

A compact version of the Schiffman phase shifter was introduced in [8]. Although the proposed design uses a smaller area and it is a cost-effective one compared with the original design, it has a narrow bandwidth.

Tresselt explained a different design procedure using a continuously tapered coupled section [9]. He noticed that the spread in coupling values between adjacent sections of the cascaded edge-coupled phase shifters, such as in [4], is large enough to produce significant reactive discontinuities in practical transverse electromagnetic line geometries, adversely affecting the phase accuracy of the devices. Tresselt described a design that could alleviate that effect by employing coupling, which is continuously tapered through the length of the device.

Manuscript received March 13, 2007; revised May 29, 2007. This work was supported by the University of Queensland under a Postdoctoral Research Fellowship.

The author is with the School of Information Technology and Electrical Engineering, The University of Queensland, St. Lucia QLD4072, Australia (e-mail: abbosh@itee.uq.edu.au).

Color versions of one or more of the figures in this paper are available online at http://ieeexplore.ieee.org.

Digital Object Identifier 10.1109/TMTT.2007.904051

He designed and constructed a phase shifter for broadband applications. However, the results indicated that the interconnecting strap parasitics, physical transitions, and etching tolerances (due to a tight coupling requirement), limited the upper frequency band and could only be partially compensated for, thus limiting the device application to around 8.5 GHz. In [10], two couplers, designed according to the tapered coupled method, were connected in tandem to form a differential phase shifter. The design required the use of a nine-section structure for the transmission lines in addition to several impedance transformers. The results presented in the paper show an insertion loss higher than 2 dB, and a phase error that is $\pm 5^\circ$ and $\pm 10^\circ$ in the $45^\circ$ and $90^\circ$ phase shifters, respectively.

In another approach to improve performance of the edge-coupled phase shifters, Taylor and Prigel [11] used a wiggling technique to design a broadband phase shifter. The wiggled edged coupled microstrip lines were used as a means of slowing the odd-mode microwave-energy propagation velocity to equal the even-mode propagation velocity and achieve broadband operation. The results in [11] show narrowband characteristics and suggest fabrication difficulties because of the very narrow space required between the coupled lines to accomplish a good performance.

In addition to the coupled lines structures, some other methods have been used to build planar phase shifters. Ahn and Wolff [12] presented several asymmetric ring-hybrid phase shifters. Each consists of a ring hybrid and reflecting terminations. The measured and simulated results in [12] indicated that the proposed design does not have the broadband characteristics of the edge-coupled structures.

With the rapid growth of microwave integrated-circuit technology, the switched phase shifters have been largely investigated [13]–[15]. The main target behind this type of phase shifter is to get a wide range of phase variation using the same device. In [13], a switching network was combined with a Schiffman phase shifter to build $180^\circ$-bit phase shifter. The network is composed of a half-wavelength coupled line, and parallel eighth wavelength open and short stubs, which are shunted at the edge points of a coupled line. The measured performance of the design shows a high phase deviation $(\pm 10^\circ)$ over the band, i.e., 1.5–4.5 GHz. In [14], switching diodes were used to convert a microstrip line to a rectangular waveguide, whereas in [15], a branch line coupler controlled by a varactor diode was used. The common features of the switched phase shifters are a high insertion loss and a narrow bandwidth. In another method, a 3-D electromagnetic-bandgap woodpile was used to design a phase shifter, which is equivalent to the switched type [16]. It suffers from the same limitations of the switched type.

Three papers have recently appeared, which suggest modifications on the previously designed phase shifters to improve their performance [17]–[19]. A compensation technique was introduced in [17] and [18] to improve performance of the Schiffman phase shifter and the multistage design proposed by Shelton and Mosko [4]. Five compensating capacitors were used to improve the return-loss performance of the two circuits. The measured results indicated an improvement in the return-loss performance across the $L$-band. However, the use of the compensation technique in [17] did not increase the useful phase-stable bandwidth; actually it resulted in a 2–3-GHz bandwidth. The use of the compensation technique in [18] for the multistage phase shifter increased the insertion loss of the device. No results were given in [18] to show the effect of the additional compensating elements on the phase performance of the phase shifter.

The latest modification to the Schiffman phase shifter included altering the ground plane underneath the coupled lines [19]. The ground plane under the coupled lines was removed; meanwhile an additional isolated rectangular conductor was placed under the coupled lines to act as a capacitor. This modification enabled the designer to build a compact phase shifter (dimension $\approx$ 3 cm $\times$ 4 cm). The measured results for this device show that it covers a 2 : 1 frequency band with better than 12-dB return loss and a moderate phase imbalance $(\pm 5^\circ)$. It still has the problem of a need for a narrow gap between the coupled lines, especially at the high-frequency range of the ultra-wideband (UWB). Moreover, the bandwidth coverage of the device indicates that it cannot be used for UWB application where the band extends from 3.1 to 10.6 GHz (3.42 : 1 band).

For the edge-coupled structure, which was used by most of the previously mentioned designs, the coupling factor is largely dependent on the gap between the two coupled lines and the dielectric constant of the substrate. Therefore, the edge-coupled phase shifters are very difficult to be fabricated using microstrip lines on printed circuit board technology for UWB applications, as the gap between the coupled lines must be very narrow to obtain a tight coupling.

In a previous study by the author to build directional couplers [20], it was noticed that broadside coupling can achieve UWB characteristics without fabrication difficulties compared with edge coupling. The work presented here adopts the broadside coupling strategy using an elliptical coupled structure in the design of UWB phase shifters. There are many challenges that are addressed in this paper: how to build a two-port broadside-coupled phase shifter with minimum insertion loss and maximum return loss across the 3.1-10.6-GHz band; how to derive a theoretical model, which shows the relation between the phase shift and the coupling factor; and how to achieve a constant phase shift across the UWB.

The proposed method in this paper exploits broadside coupling between top and bottom elliptical microstrip patches via an elliptical slot located in the mid layer, which forms the ground plane. Variations of the phase shift, return loss, and insertion loss of the device with the coupling factor are calculated using a simple theoretical model. The model shows that it is possible to design high-performance UWB phase shifters for the $25^\circ$–$48^\circ$ range using the suggested structure. The proposed method is used to design $30^\circ$ and $45^\circ$ phase shifters that have compact size. The simulated and measured results show that the designed phase shifters achieve better than $\pm 3^\circ$ phase stability, less than 1-dB insertion loss, and better than 10-dB return loss across the UWB, i.e., 3.1–10.6 GHz. In addition to that, the presented device has a simple structure, which can be easily manufactured.

## II. Analysis

The analysis used in this paper follows the conventional approach adopted for the coupled microstrip lines [21]–[24]. The phase shifter is considered as a four-port device with two of its

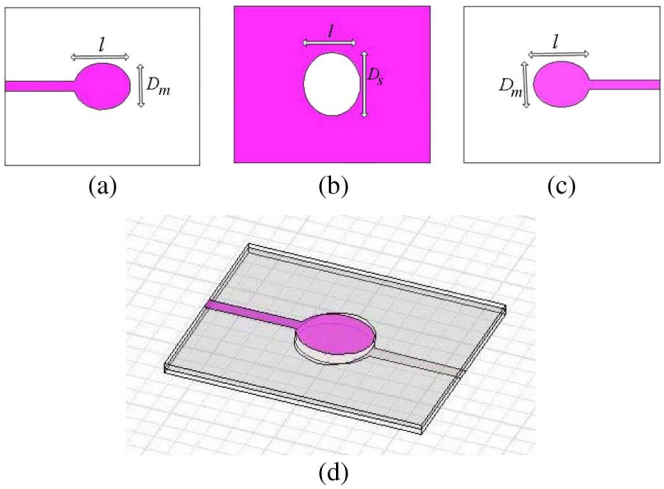


Fig. 1. Configuration of the proposed phase shifter. (a) Top layer. (b) Mid layer. (c) Bottom layer. (d) Whole structure.

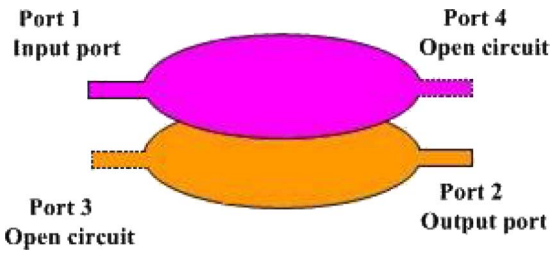


Fig. 2. Proposed phase shifter as a four-port device with two of the ports open circuited.

ports open circuited. The other two ports are the input and output ports. The performance of the phase shifter is defined in terms of the return loss, insertion loss, and the differential phase shift. To calculate (or measure) the phase-shift performance of the device, a comparison is made with a reference mictrostrip transmission line with 50-Ω impedance.

Configuration of the proposed multilayer phase shifter is shown in Fig. 1. It consists of two elliptical microstrip patches, which are connected to the input and output microstrip lines, facing each other at the top and bottom layers. The coupling between these patches is achieved via an elliptical slot in the ground plane, which is located at the mid layer. The elliptical shape for the coupled structure is chosen because of its ability to achieve an almost constant coupling factor over the UWB.

The analysis starts by considering the phase shifter as a four-port backward coupler with two of the output ports terminated in an open circuit (see Fig. 2).

Assume the device is designed to have a coupling equal to $C$ between the top and bottom patches and that the input and output signals to/from the $i$th port are $a_i$ and $b_i$, respectively. Depending on odd–even modes analysis of the four-port coupler, the output signals at Port 1 (the input port) and Port 2 (the output port) can be calculated as follows [21]–[24]:

$$b_1 = \frac{jC\sin(\beta_{ef}l)a_3 + \sqrt{1-C^2}a_4}{\sqrt{1-C^2}\cos(\beta_{ef}l) + j\sin(\beta_{ef}l)} \quad (1)$$

$$b_2 = \frac{jC\sin(\beta_{ef}l)a_4 + \sqrt{1-C^2}a_3}{\sqrt{1-C^2}\cos(\beta_{ef}l) + j\sin(\beta_{ef}l)} \quad (2)$$

where $l$ is the physical length of the coupled structure and $\beta_{ef}$ is the effective phase constant in the medium of the coupled structure. For the structure under investigation, it is possible to show that

$$\beta_{ef} = \frac{\beta_e + \beta_o}{2} = 360^\circ \times \sqrt{\varepsilon_r}/\lambda \quad (3)$$

where $\beta_e$ and $\beta_o$ are the phase constants for the even and odd modes, respectively, $\lambda$ is the free-space wavelength, and $\varepsilon_r$ is the dielectric constant of the substrate.

Assuming that the output port (Port 2) is perfectly matched, then the incident (= reflected) signals at ports 3 and 4 are

$$b_3 = \frac{jC\sin(\beta_{ef}l)a_1}{\sqrt{1-C^2}\cos(\beta_{ef}l) + j\sin(\beta_{ef}l)} \quad (4)$$

$$b_4 = \frac{\sqrt{1-C^2}a_1}{\sqrt{1-C^2}\cos(\beta_{ef}l) + j\sin(\beta_{ef}l)}. \quad (5)$$

As ports 3 and 4 are terminated in an open circuit, then the reflection coefficient at those ports is equal to 1. Therefore, $a_3 = b_3$ and $a_4 = b_4$. Using this conclusion in (1)–(5),

$$S_{11} = \frac{1 - C^2\left(1 + \sin^2(\beta_{ef}l)\right)}{\left[\sqrt{1-C^2}\cos(\beta_{ef}l) + j\sin(\beta_{ef}l)\right]^2} \quad (6)$$

$$S_{21} = \frac{j2C\sqrt{1-C^2}\sin(\beta_{ef}l)}{\left[\sqrt{1-C^2}\cos(\beta_{ef}l) + j\sin(\beta_{ef}l)\right]^2} \quad (7)$$

where $S_{11} = b_1/a_1$ is the return loss of the input port, $S_{21} = b_2/a_1$ is the insertion loss from the input to the output port.

Phase shift of the output signal compared to the input signal can be found from (7) as follows:

$$\Phi_c = 90^\circ - 2\arctan\left[\frac{\sin(\beta_{ef}l)}{\sqrt{1-C^2}\cos(\beta_{ef}l)}\right]. \quad (8)$$

To find the differential phase shift, which can be obtained using the proposed structure, a comparison should be made with a reference transmission line. A 50-Ω microstrip line is assumed as a reference in this paper. The phase shift caused by a section of microstrip line of physical length $l_m$ is

$$\Phi_m = -\beta_m l_m = -360^\circ \times l_m\sqrt{\varepsilon_{ef}}/\lambda \quad (9)$$

where $\beta_m$ and $\varepsilon_{ef}$ are the phase constant and effective dielectric constant of the microstrip transmission line, respectively. The parameter $\varepsilon_{ef}$ can be calculated using the well-known formulas as in [25].

The differential phase shift $(\Delta\Phi)$ from (8) and (9) is

$$\Delta\Phi = 90^\circ - 2\arctan\left[\frac{\sin(\beta_{ef}l)}{\sqrt{1-C^2}\cos(\beta_{ef}l)}\right] + \beta_m l_m. \quad (10)$$

Variation of the calculated $\Delta\Phi$, using (10), for different values of the coupling length $(\beta_{ef}l)$ and coupling factor $(C)$ is shown in Fig. 3. The Rogers RO4003C (with $\varepsilon_r = 3.38$, thickness $= 0.508$ mm, and tangent loss $= 0.0023$) was assumed as the substrate.

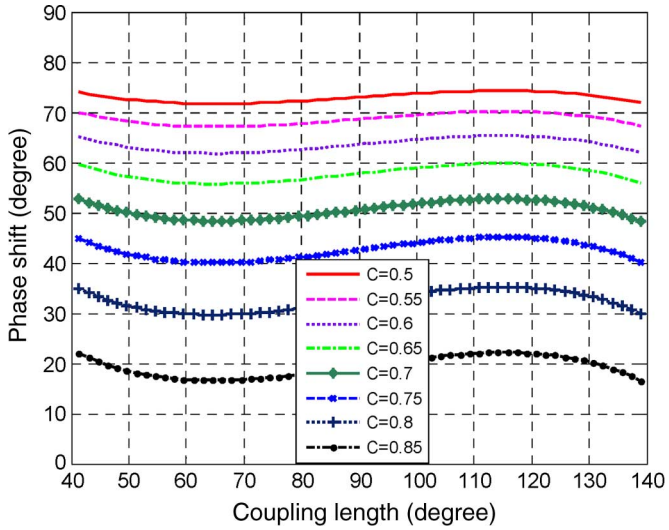


Fig. 3. Theoretical estimation of the phase variation with the coupling length for different values of the coupling factor $C$.

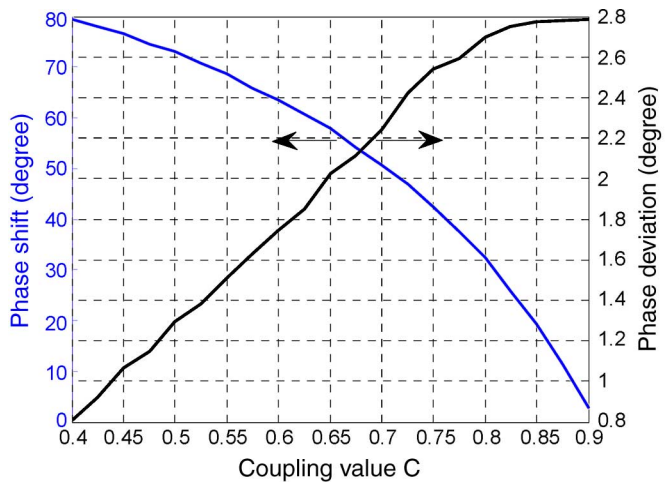


Fig. 4. Theoretical estimation for the relation between the differential phase shift $\Delta\Phi$ and phase deviation with the coupling factor $C$.

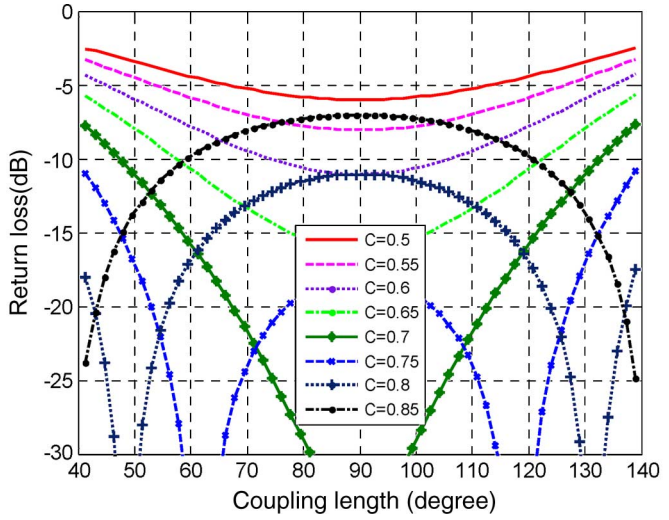


Fig. 5. Theoretical estimation of variation of the return loss with the coupling length for different values of the coupling factor $C$.

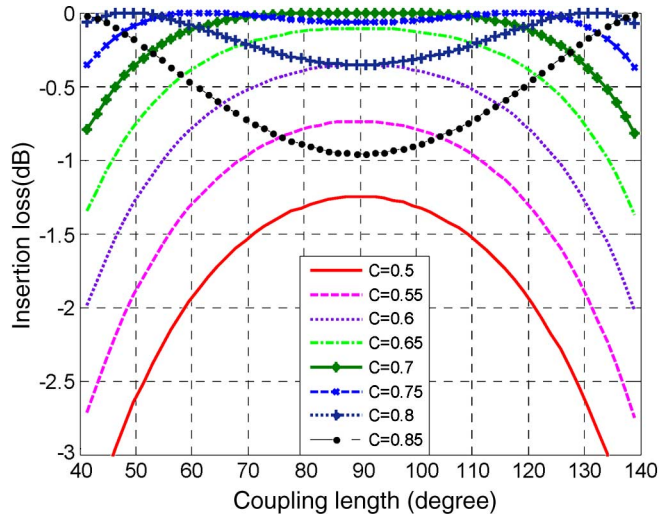


Fig. 6. Theoretical estimation of variation of the insertion loss with the coupling length for different values of the coupling factor $C$.

In Fig. 3, the physical length of the microstrip transmission line $l_m$ is optimized to obtain a minimum deviation in the differential phase shift for each value of the coupling. It was found that $l_m$ should be around $2l$, which is the total physical length of the top and bottom coupled patches.

Fig. 3 indicates an odd symmetry of $\Delta\Phi$ around the length $\beta_{ef}l = 90°$. The results in Fig. 3 also reveal that it is possible to design a phase shifter with wide range of phase shift by varying value of the coupling factor $C$. The estimated phase range using (10) extends from 0° to 90° for $C$ from 1 down to 0. There are still two parameters to be checked before judging performance of the device: the return loss and insertion loss.

According to the results shown in Fig. 3, there is an inverse relation between $\Delta\Phi$ and $C$. This conclusion is verified by plotting in Fig. 4 the average value of $\Delta\Phi$ and the phase deviation (with respect to the average value) with $C$ using the data of Fig. 3. It is also obvious from this figure that the maximum phase deviation around the nominal value of $\Delta\Phi$ has a direct proportional relationship with $C$.

Designing a high-performance phase shifter not only requires phase stability with the least deviation around the nominal value across the required bandwidth, but it also requires that the device should have a low insertion loss and a high return loss across that band. Variation of the return loss and insertion loss with the coupling length are shown in Figs. 5 and 6 for different values of the coupling factor by using the absolute value of the parameters in (6) and (7).

It is clear from Figs. 5 and 6 that there is an even symmetry of the return loss and insertion loss around the point $\beta_{ef}l = 90°$. Hence, to achieve the best performance (low insertion loss and high return loss) over a broad band, $\beta_{ef}l$ should be equal to 90° at the center frequency of operation.

Referring to Figs. 5 and 6, it is important to make sure which values of $C$ give an acceptable performance over the UWB from 3.1 to 10.6 GHz. As mentioned earlier, the length of the coupled structure must be 90° at the center frequency, which is $(3.1 + 10.6)/2 = 6.85$ GHz. Assuming the physical length

of the coupled structure $l$ is constant, then the coupling length $\beta_{ef}l$ is equivalent to $90^\circ \times 3.1/6.85 = 40.7^\circ$ at 3.1 GHz and $90^\circ \times 10.6/6.85 = 139.3^\circ$ at 10.6 GHz. According to Figs. 5 and 6, the return loss is more than 10 dB and the insertion loss is less than 0.5 dB across the whole UWB (3.1–10.6 GHz) when $0.72 \leq C \leq 0.82$.

From Fig. 4, it seems that it is possible to design high-performance 25°–48° phase shifters that cover the 3.1–10.6-GHz band using the proposed model with $0.72 \leq C \leq 0.82$. A multistage phase shifter can be designed to achieve a higher range of differential phase shift when required. If, in some applications, the required bandwidth is less than the one used in this paper, other ranges of phase shifts are possible with the presented method using only one stage.

## III. Design

In order to establish the validity of the proposed method, 30° and 45° phase shifters were designed using the following steps. From Fig. 4, the coupling should be 0.81 and 0.73 for the 30° and 45° phase shifter, respectively. The return loss, from Fig. 5, is higher than 12 and 10 dB for the 30° and 45° phase shifter, respectively, across the 3.1–10.6-GHz band. The insertion loss is less than 0.4 and 0.5 dB for the 30° and 45° phase shifter, respectively, across the same band (see Fig. 6).

Depending on value of the coupling, the even $(Z_{oe})$ and odd $(Z_{oo})$ mode characteristic impedances for the coupled patches are calculated using the following equations:

$$Z_{oe} = Z_o\sqrt{\frac{1+C}{1-C}} \quad Z_{oo} = Z_o\sqrt{\frac{1-C}{1+C}} \tag{11}$$

where $Z_o(= 50\ \Omega)$ is the characteristic impedance of the microstrip ports of the coupler. Using $C = 0.81$ for the 30° phase shifter, the impedances $Z_{oe}$ and $Z_{oo}$ can be found to be 154.3 and 16.2 Ω, respectively. If the device is designed to have 45° phase shift, $Z_{oe}$ and $Z_{oo}$ can be calculated to be 126.6 and 19.8 Ω, respectively. To determine dimension of the coupled region, which gives these impedance values, it is possible to use the following equations [26]:

$$Z_{oe} = \frac{60\pi}{\sqrt{\varepsilon_r}}\frac{K(k_1)}{K'(k_1)} \quad Z_{oo} = \frac{60\pi}{\sqrt{\varepsilon_r}}\frac{K'(k_2)}{K(k_2)} \tag{12}$$

where $\varepsilon_r$ is the dielectric constant of the substrate, $K(k)$ is the first kind elliptical integral, and $K'(k) = K(\sqrt{1-k^2})$. The parameters $k_1$ and $k_2$ are used to find the major diameters of the elliptical coupled microstrip at the top and bottom layers $(D_m)$ and slot $(D_s)$ at the mid layer according to the following equations [20]:

$$k_1 = \sqrt{\frac{\sinh^2(\pi^2 D_s/(16h))}{\sinh^2(\pi^2 D_s/(16h)) + \cosh^2(\pi^2 D_m/(16h))}} \tag{13}$$

$$k_2 = \tanh\left(\pi^2 D_m/(16h)\right) \tag{14}$$

Physical length (secondary diameter) of the elliptical microstrip/slot coupled structures $(l)$ must be chosen to be equal to a quarter of the effective wavelength at the center frequency of operation, i.e., at 6.85 GHz, as proven according to Figs. 3 and 4. It is to be noted that the coupling factor $C$ was considered constant when calculating each set of results shown in Figs. 3, 5, and 6. However, the measured results for the directional couplers in [20], which used a broadside coupled structure similar to the one used in this paper, show that the coupling factor $C$ tends to be lower at the two ends of the frequency band compared with its value at the center frequency. If this effect is included into the results shown in Fig. 4, the designed device is going to have a higher average phase shift at the two ends compared with its value at the center frequency. On the other hand, Fig. 3 shows that, for a certain value of the coupling, $\Delta\Phi$ is larger than the average value at the lower frequency band and smaller at the upper frequency band. The combination of these two factors results in a worse performance at the lower end and a better performance at the upper end of the frequency band. Therefore, it is better to design the phase shifter with a length that is larger than 90° at the center frequency. A comparative study of the mode of variation of $\Delta\Phi$ (from Fig. 3) and measured $C$ (from [20]) with frequency indicated that the widest bandwidth can be achieved when the coupling length $\beta_{ef}l \approx 110^\circ$ at a center frequency of 6.85 GHz.

TABLE I
Calculated and Optimized Values of the Design Parameters

| Parameter value (mm) | | $D_m$ | $D_s$ | $l$ |
|---|---|---|---|---|
| 30° Phase Shifter | Calculated | 5.6 | 8.4 | 7.2 |
| | Optimized | 5.9 | 8.1 | 7.25 |
| 45° Phase Shifter | Calculated | 4.9 | 7.5 | 7.2 |
| | Optimized | 4.75 | 7.3 | 7.1 |

The last step in the design procedure is to find width $(w_m)$ of the reference line and the microstrip lines that connect the phase shifter to the 50-Ω input/output ports. This can be achieved using the standard microstrip design equations [25].

Dimension of the phase shifters calculated using the proposed method are shown in Table I. The phase shifters were assumed to use a Rogers RO4003C as a substrate. Table I also shows the final dimension after fine tuning using the optimization capability of the full electromagnetic software package Ansoft HFSSv10. There is a little difference (less than 5%) between the calculated and optimized values. This gives a high credibility to accuracy of the proposed method.

## IV. Results and Discussions

To prove the validity of the presented design method, the 30° and 45° phase shifters designed in Section III and aimed for the operation in the 3.1–10.6-GHz frequency band were manufactured and tested. A Rogers RO4003C, with 17-$\mu$m-thick conductive coating, is selected for the devices development. A photograph for one of the manufactured phase shifters is shown in Fig. 7. Dimension of the phase shifter alone (excluding the reference transmission line) is 2.5 cm × 2 cm. This reveals compactness of the proposed phase shifter.

It is to be noted that, in the manufactured devices, the coupled structure of physical length $l$ and the reference transmission line of physical length $l_m$ are connected to the input/output subminiature A (SMA) connectors using the same additional length of microstrip transmission lines.

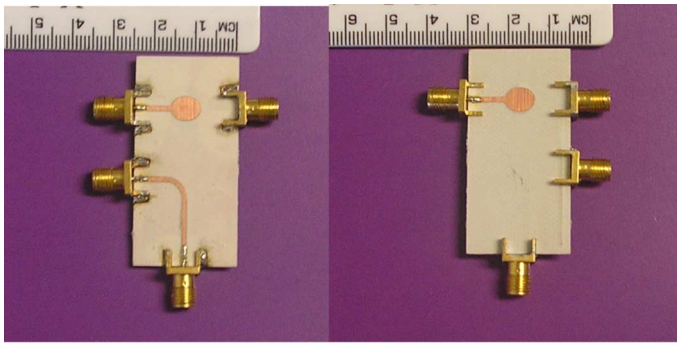

(a) (b)

Fig. 7. One of the manufactured phase shifters. (a) Top layer. (b) Bottom layer. The upper part of (a) and (b) is the phase shifter, whereas the reference transmission line is shown at the lower part of (a).

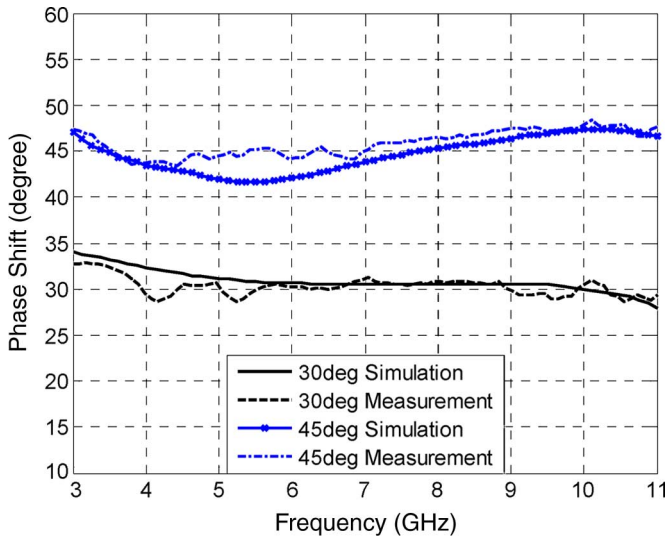


Fig. 8. Simulated and measured differential phase shift for the two developed phase shifters.

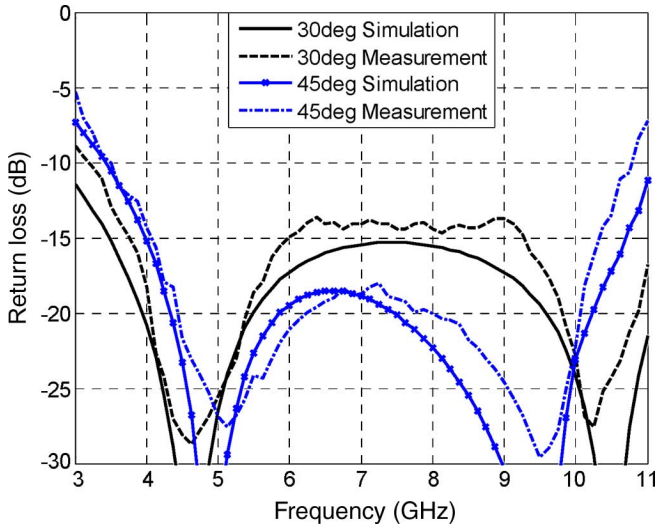


Fig. 9. Simulated and measured return loss for the two developed phase shifters.

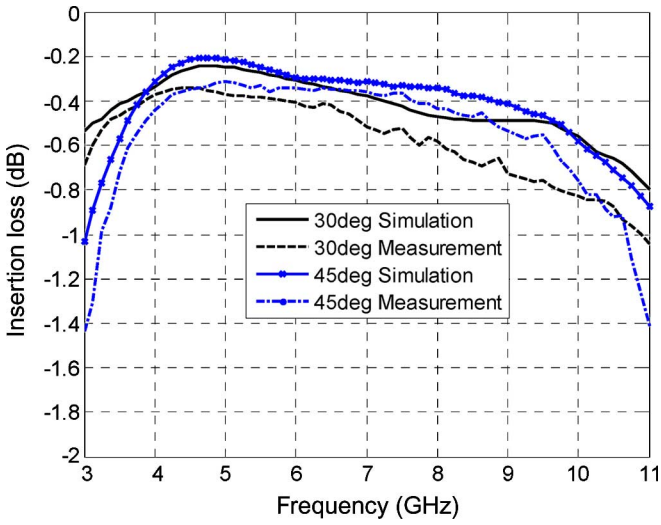


Fig. 10. Simulated and measured insertion loss for the two developed phase shifters.

The differential phase shift $(\Delta\Phi)$, return loss, and insertion loss of the designed devices were first verified using the Ansoft HFSSv10 software and then measured using a vector network analyzer. The simulated and measured $\Delta\Phi$ of the designed $30^\circ$ and $45^\circ$ phase shifters are shown in Fig. 8. It is clear that the designed phase shifter features UWB characteristics. The value of $\Delta\Phi$ is $30^\circ \pm 3^\circ$ in the simulations and $30^\circ \pm 2.5^\circ$ according to the measured results for the $30^\circ$ phase shifter across the 3.1–10.6-GHz band. For the $45^\circ$ phase shifter, $\Delta\Phi$ is $45^\circ \pm 3^\circ$ in the simulation and $45^\circ \pm 2.3^\circ$ according to the measured results across the same UWB. Fig. 8 indicated that the measured results are close to the simulated results, and both of them are in good agreement with the theoretical prediction shown in Fig. 4, which gives an estimation of $30^\circ \pm 2.7^\circ$ and $45^\circ \pm 2.4^\circ$ for the differential phase shift for the two phase shifters. The general shape of differential phase variation with frequency is also in good agreement with results of the theoretical analysis shown in Fig. 3.

The combined effect of using a coupling length equal to $110^\circ$ (instead of $90^\circ$) and the nonconstant value of $C$ on $\Delta\Phi$ can be seen in Fig. 8. The measured value of $\Delta\Phi$ at the lower frequency band is almost equal to its value at the higher frequency band for the $45^\circ$ phase shifter. In the case of the $30^\circ$ phase shifter, $\Delta\Phi$ is almost constant during most of the frequency band.

The simulated and measured return loss for the $30^\circ$ phase shifter is better than 12 dB according to the simulations and better than 10 dB in the measured results across the whole UWB (see Fig. 9). It is always better than 15 dB in the 3.7–11-GHz band. Concerning the $45^\circ$ phase shifter, the return loss is better than 10 dB in the 3.3–10.6-GHz band, as shown in Fig. 9. The return loss of this phase shifter is always better than 18 dB in the 4.2–10.2-GHz band. There is a good agreement between the measured and simulated results shown in Fig. 9 and the theoretical estimation shown in Fig. 5, except a little discrepancy at the lower part of the frequency band, i.e., around 3 GHz. This discrepancy can be justified by the combined effect of using a longer coupled structure and the nonconstant value of $C$.

In Fig. 10, the simulated and measured insertion loss for the $30^\circ$ and $45^\circ$ phase shifters is shown. The simulated insertion loss for the $30^\circ$ phase shifter is better than 0.6 dB, whereas it

is better than 0.85 dB according to the measured results in the 3.1–10.6-GHz band. Concerning the 45° phase shifter, the simulated and measured insertion loss is better than 0.8 and 1 dB, respectively, across the 3.1–10.6-GHz band, as shown in Fig. 10.

There is a little difference between the measured and simulated results shown in Fig. 10. The measured insertion loss is more than the simulated value by approximately 0.15 dB, on average, for the two phase shifters. This additional insertion loss comes from the two SMA connectors, which were used in the measurements, but not included in the simulations. According to the data sheet of the used connectors, their insertion loss increases with frequency and becomes more than 0.1 dB per connector after 6 GHz.

## V. Conclusion

Simple and clear guidelines have been presented to design compact planar phase shifters with UWB characteristics. The proposed method exploits broadside coupling between top and bottom elliptical microstrip patches via an elliptical slot located in the mid layer, which forms the ground plane. A theoretical model has been used to analyze performance of the proposed devices. The model has shown that it is possible to design high-performance UWB phase shifters for the 25°–48° range using the proposed structure. The design method has been used to design 30° and 45° phase shifters, which have compact size, i.e., 2.5 cm × 2 cm. The simulated and measured results have shown that the designed phase shifters have better than ±3° phase stability, less than 1-dB insertion loss, and better than 10-dB return loss across the UWB from 3.1 to 10.6 GHz.

The UWB behavior, compactness, and easy of fabrication of the presented phase shifters should attract considerable interest from designers of wireless systems, in general, and UWB systems, in particular.

The multilayer broadside-coupled configuration of the proposed device is especially suitable for implementation in modern multilayer structures such as the laminated multichip modules (MCMs-L) and low temperature co-fired ceramics (LTCC). In such structures, broadside coupling is much preferred from a reproducibility and loss perspective.

## References


[1] B. Schiffman, "A new class of broadband microwave 90-degree phase shifters," *IRE Trans. Microw. Theory Tech.*, vol. MTT-6, no. 4, pp. 232–237, Apr. 1958.

[2] C. Free and C. Aitchison, "Improved analysis and design of coupled-line phase shifters," *IEEE Trans. Microw. Theory Tech.*, vol. 43, no. 9, pp. 2126–2131, Sep. 1995.

[3] B. Schiffman, "Multisection microwave phase-shift network," *IEEE Trans. Microw. Theory Tech.*, vol. 14, no. 4, p. 209, Apr. 1966.

[4] J. Shelton and J. Mosko, "Synthesis and design of wideband equal-ripple TEM directional couplers and fixed phase shifters," *IEEE Trans. Microw. Theory Tech.*, vol. MTT-14, no. 10, pp. 246–252, 462–473, Oct. 1966.

[5] V. Meschanov, I. Metelnikova, V. Tupikin, and G. Chumaevskaya, "A new structure of microwave ultrawide-band differential phase shifter," *IEEE Trans. Microw. Theory Tech.*, vol. 42, no. 5, pp. 762–765, May 1994.

[6] B. Schiek and J. Kohler, "A method for broadband matching of microstrip differential phase shifters," *IEEE Trans. Microw. Theory Tech.*, vol. MTT-25, no. 8, pp. 666–671, Aug. 1977.

[7] J. Quirarte and J. Starski, "Novel Schiffman phase shifters," *IEEE Trans. Microw. Theory Tech.*, vol. 41, no. 1, pp. 9–14, Jan. 1993.

[8] D. Chai, M. Linh, M. Yim, and G. Yoon, "Asymmetric Teflon-based Schiffman phase shifter," *Electron. Lett.*, vol. 39, no. 6, pp. 529–530, 2003.

[9] C. Tresselt, "Broad-band tapered-line phase shift networks," *IEEE Trans. Microw. Theory Tech.*, vol. MTT-16, no. 1, pp. 51–52, Jan. 1968.

[10] F. Minnaar, J. Coetzee, and J. Joubert, "A novel ultrawideband microwave differential phase shifter," *IEEE Trans. Microw. Theory Tech.*, vol. 45, no. 8, pp. 1249–1252, Aug. 1997.

[11] J. Taylor and D. Prigel, "Wiggly phase shifters and directional couplers for radio-frequency hybrid-microcircuit applications," *IEEE Trans. Parts, Hybrids, Packag.*, vol. PHP-12, no. 4, pp. 317–323, Dec. 1976.

[12] H. Ahn and I. Wolff, "Asymmetric ring-hybrid phase shifters and attenuators," *IEEE Trans. Microw. Theory Tech.*, vol. 50, no. 4, pp. 1146–1155, Apr. 2002.

[13] S. Eom, "Broadband 180 ° bit phase shifter using $\lambda/2$ coupled line and parallel $\lambda/8$ stubs," *IEEE Microw. Wireless Compon. Lett.*, vol. 14, no. 5, pp. 228–230, May 2004.

[14] Z. Jin, S. Ortiz, and A. Mortazawi, "Design and performance of a new digital phase shifter at $X$-band," *IEEE Microw. Wireless Compon. Lett.*, vol. 14, no. 9, pp. 428–430, Sep. 2004.

[15] S. Cheng, E. Öjefors, P. Hallbjörner, and A. Rydberg, "Compact reflective microstrip phase shifter for traveling wave antenna applications," *IEEE Microw. Wireless Compon. Lett.*, vol. 16, no. 7, pp. 413–433, Jul. 2006.

[16] A. Weily, T. Bird, K. Esselle, and B. Sanders, "Woodpile EBG phase shifter," *Electron. Lett.*, vol. 42, no. 25, pp. 1463–1464, Dec. 2006.

[17] S. Gruszczynski, K. Wincza, and K. Sachse, "Design of compensated coupled-stripline 3-dB directional couplers, phase shifters, and magic-T's—Part I: Single-section coupled-line circuits," *IEEE Trans. Microw. Theory Tech.*, vol. 54, no. 11, pp. 3986–3994, Nov. 2006.

[18] S. Gruszczynski, K. Wincza, and K. Sachse, "Design of compensated coupled-stripline 3-dB directional couplers, phase shifters, and magic-T's—Part II: Broadband coupled-line circuits," *IEEE Trans. Microw. Theory Tech.*, vol. 54, no. 9, pp. 3501–3507, Sep. 2006.

[19] Y. Guo, Z. Zhang, and L. Ong, "Improved wideband Schiffman phase shifter," *IEEE Trans. Microw. Theory Tech.*, vol. 54, no. 3, pp. 1196–1200, Mar. 2006.

[20] A. Abbosh and M. Bialkowski, "Design of compact directional couplers for UWB applications," *IEEE Trans. Microw. Theory Tech.*, vol. 55, no. 2, pp. 189–194, Feb. 2007.

[21] H. Riblet, "A mathematical theory of directional couplers," *Proc. IRE*, vol. 35, no. 11, pp. 1307–1313, Nov. 1947.

[22] B. Oliver, "Directional electromagnetic couplers," *Proc. IRE*, vol. 42, no. 11, pp. 1686–1692, Nov. 1954.

[23] E. Jones and J. Bolljahn, "Coupled-strip transmission line filters and directional couplers," *IEEE Trans. Microw. Theory Tech.*, vol. 4, no. 2, pp. 75–81, Feb. 1956.

[24] J. Reed and G. Wheeler, "A method of analysis of symmetrical four-port networks," *IEEE Trans. Microw. Theory Tech.*, vol. MTT-4, no. 4, pp. 246–252, Apr. 1956.

[25] D. Pozar, *Microwave Engineering*, 3rd ed. New York: Wiley, 2005.

[26] M. Wong, V. Hanna, O. Picon, and H. Baudrand, "Analysis and design of slot-coupled directional couplers between double-sided substrate microstrip lines," *IEEE Trans. Microw. Theory Tech.*, vol. 39, no. 12, pp. 2123–2128, Dec. 1991.


**Amin M. Abbosh** was born in Mosul, Iraq. He received the M.Sc. degree in communication systems and Ph.D. degree in microwave engineering from Mosul University, Mosul, Iraq, in 1991 and 1996, respectively.

Until 2003, he was Head of the Information Engineering Department, Mosul University. In 2004, he joined the Centre for Wireless Monitoring and Applications, Griffith University, as a Post-Doctoral Research Fellow. He is currently a Research Fellow with the School of Information Technology and Electrical Engineering, The University of Queensland, St. Lucia, Australia. His research interests include antennas, radio-wave propagation, microwave devices, and design of UWB wireless systems.